Ocean Engineering 125 (2016) 38–50

Contents lists available at ScienceDirect

Ocean Engineering

journal homepage: www.elsevier.com/locate/oceaneng

3D experimental study on a cylindrical floating breakwater system

Chun-Yan Ji [a], Yu-Chan GUO [a], Jie Cui [a], Zhi-Ming Yuan [a,b,*], Xiao-Jian Ma [a]

[a] School of Naval Architecture and Ocean Engineering, Jiangsu University of Science and Technology, Zhenjiang 212003, China
[b] Department of Naval Architecture, Ocean and Marine Engineering, University of Strathclyde, Glasgow, UK

ARTICLE INFO

Article history:
Received 1 January 2016
Received in revised form
8 July 2016
Accepted 22 July 2016
Available online 10 August 2016

Keywords:
Floating breakwater system
3D experimental study
Wave transmission coefficient
Wave reflection coefficient
Wave dissipation coefficient
Motion responses

ABSTRACT

The objective of the present study is to investigate the performance of a cylindrical floating breakwater system based on 3D experimental tests. The experiments were carried out in the wave basin (36 m*60 m*1.5 m)of the Ocean University of China. The cylindrical floating breakwater system consists of 10cylindrical floating breakwater units and 10mesh cages with balls in them, connected by 18 connectors and moored by a taut mooring system. The wave transmission coefficients, reflection coefficients, dissipation coefficients and motion responses of the floating breakwater are measured in both oblique and beam sea conditions. It is found that with the increase of the wavelength, both of the wave transmission coefficients and motion response amplitude of the FB system suffers an increase before it reaches its peak value, followed by a decrease trend. It can be concluded from the experiments that the proposed FB system has a satisfactory performance and it can be used to a wide range of sea conditions.

1. Introduction

The floating breakwaters (FBs) have been extensively studied in the last few decades. These studies focus on different types of the floating breakwaters, such as cylindrical type (Ozeren et al., 2011), single pontoon type, double pontoon type, broad-net type (Dong et al., 2008), box type, Π shape (Gesraha, 2006) so on. Floating breakwaters attenuate waves mainly in two ways: (1) reflecting waves; (2) disturbing the motions of the wave particles. Compared to the traditional breakwater, the floating breakwater has many advantages: (1) Environment friendly: FB will not block the ocean flow and the ecosystem can be protected; (2) Economy: FB is more economical than traditional breakwater, especially in deep water; (3) Feasibility: FB has lower requirement of seabed condition and it is easy to be installed; (4) The floating body, mooring line and anchor are easy to be manufactured. In addition, the existence of specific environmental design parameters, such as poor foundation and deep water conditions, water circulation and esthetic considerations, enhanced the utilization of floating breakwater (McCartney, 1985).

In order to investigate the efficiency of wave attenuation of different types of floating breakwaters, many experiments studies have been carried out. Arunachalam and Raman (1982) conducted a two-dimensional model study to investigate the transmission coefficient of a horizontal floating plate breakwater. Bayram (2000) evaluated the performance of a sloping float breakwater by a two-dimensional model study. Stamos et al. (2003) conducted a 2D experimental study to compare the reflection and transmission characteristics of submerged hemi-cylindrical and rectangular rigid and water-filled flexible breakwater models. Ragih et al. (2006) carried out a 2D experiment to investigate the wave attenuate by using spherical floating bodies. Martinelli et al. (2008) carried out a 3D experiment to study the effect of different layouts of floating breakwaters on wave transmission, loads along moorings and connectors, under oblique waves. Dong et al. (2008) measured the wave transmission coefficients of three types of breakwaters under regular waves with or without currents by a two-dimensional physical model tests. Wang and Sun (2010) conducted a 2D experimental study to investigate the hydrodynamic efficiency of a porous floating breakwater. Ozeren et al. (2011) conducted a laboratory investigation of the hydrodynamic interaction of cylindrical breakwaters with monochromatic waves in deep and transitional water depths. Peña et al. (2011) investigated wave transmission coefficient, mooring lines and module connector forces with four different designs of floating breakwaters by 2D and 3D physical model tests. He et el. (2012) investigated the hydrodynamic performance of floating breakwaters with and without pneumatic chambers in a wave flume. Koraim and Rageh (2013) studied the hydrodynamic efficiency (the wave transmission, reflection, and energy dissipation coefficients) of a floating breakwater system, which consists of a rectangular box and a series of

* Corresponding author. Dep. of Naval Architecture, Ocean & Marine Engineering, University of Strathclyde. Henry Dyer Building, G4 0LZ, Glasgow, UK.
Tel: +44 (0)141 548 3308. Fax: +44 (0)141 552 2879.
E-mail address: zhiming.yuan@strath.ac.uk (Z.-M. Yuan).

http://dx.doi.org/10.1016/j.oceaneng.2016.07.051
0029-8018/

plates, by a 2D experiment. Loukogeorgaki et al. (2014) conducted a 3D experimental investigation for assessing the wave attenuation effectiveness of a FB, consisting of an array of multiple floating box-type modules, under the action of perpendicular and oblique regular and irregular waves.

The performance of the floating breakwaters has also been studied theoretically and numerically. Williams and Abul-Azm (1997) theoretically investigated the hydrodynamic properties of a dual pontoon floating breakwater consisting of a pair of floating cylinders of rectangular section, connected by a rigid deck. Gesraha (2006) investigated the reflection and transmission of incident waves interacting with a Π shaped floating breakwater by an eigenfunction expansion method. Chen et al. (2012) theoretically studied the hydrodynamic behaviors of a floating breakwater consisting of a rectangular pontoon and horizontal plates. Loukogeorgaki et al. (2012) numerically investigated the hydroelastic performance of a free, flexible, mat-shaped floating breakwater that consists of a grid of flexible floating modules connected flexibly in both horizontal directions. The investigation had been conducted in the frequency domain under the action of oblique incident waves. Peng et al. (2013) studied the interactions of waves with submerged floating breakwaters moored by inclined tension legs, using a numerical wave tank model which based on the Navier–Stokes solver. Koraim (2015) mathematically and experimentally investigated the hydrodynamic characteristics of the semi immersed caissons breakwater supported by two rows of piles.

FB's oscillating motion will generate the radiation waves. The waves propagate upstream can be regarded as a way to attenuate incoming wave energy. Therefore the motion response is another important factor of assessing a floating breakwater configuration. By using the finite element method (FEM), Hanif (1983) analyzed hydrodynamic properties of an elliptical cylinder floating breakwater in heaving and swaying motions. Sannasiraj et al. (1998) conducted a 2D experimental and theoretical investigation to study the motion responses and mooring forces of a pontoon-type FB for different mooring line configurations. Rahman et al. (2006) developed a numerical model by using the volume of fluid (VOF) method as well as 2D experimental studies to estimate the nonlinear dynamics of a pontoon type moored submerged breakwater under wave action for both the vertical and inclined mooring alignments. Najafi-Jilani, Rezaie-Mazyak. (2011) numerically analyzed the movement pattern of a floating breakwater, using Smoothed Particle Hydrodynamic (SPH) method as a Lagrangian scheme. Sannasiraj et al. (1995), Abul-Azm and Gesraha (2000), Loukogeorgaki and Angelides (2005), Zheng et al. (2006) and Gesraha (2006) also had investigated the dynamic response of floating breakwaters under the action of incident oblique waves.

It can be found that most of the researchers investigated floating breakwaters by two-dimensional model experiments. However, compared with 3D basin experiment, 2D wave tank experiment can only obtain part of dynamic characteristics and wave dissipation performance of a floating breakwater in beam waves. In fact, the floating breakwater system usually consists of an array of multiple floating units which are connected by rigid or flexible connectors and moored by mooring lines. Therefore, the motion response of a 3D FB system is a coupled dynamics problem and the energy dissipation performance of the system is more complicated than that of the 2D model. Even though there are some studies on the performance of the floating breakwaters which consists of an array of multiple floating units, the 3D experimental studies are still required to investigate the hydrodynamic behaviors of the floating breakwater system. The present FB system consists of 10 traditional cylindrical FB units, 18 elastic connectors, ten mesh cages and 12,000 balls, and it is moored by 64 mooring lines. This scaled system represents the real physical model which is to be used in engineering practice. For such a complicated floating breakwater system, no single experimental study yet has been conducted to explore its wave attenuation performance. Therefore, the experimental procedure, as well as the findings acquired from the tests will be of benefit for the researchers to have a better understanding of the coupled behavior between multiple floating bodies.

Ji et al. (2015) conducted a 2D experiment to study a new type of floating breakwater. Comparing the four models' capacity of wave attenuation, Model 3 (the traditional cylindrical FB with a mesh cage and balls) is the best configuration. Based on Ji et al. (2015), the present paper conducted a 3D hydrodynamic experiment to investigate the hydrodynamic efficiency (wave transmission coefficients, reflection coefficients, and energy dissipation coefficients) and motion responses (surge, sway, heave, roll, pitch and yaw motion) of a floating breakwater system within the action of both beam and oblique wave as a function of wave period and wave height separately.

2. Cylindrical floating breakwater introduction

According to Ji et al. (2015), the main structure of a traditional cylindrical FB includes eleven cylinders, which are made of reinforced concrete. Two of them have the size of 4 m (diameter)*15.2 m (length), while the others are 0.4 m*2 m. Nighty eight percent of the wave energy is transmitted underneath the water surface, to disturb particle orbit and reduce the cost, a mesh cage with the length of 15.2 m and the width of 2 m was hanged blow the main structure. In order to enhance the dissipation of wave energy, 1200 rubber hollow

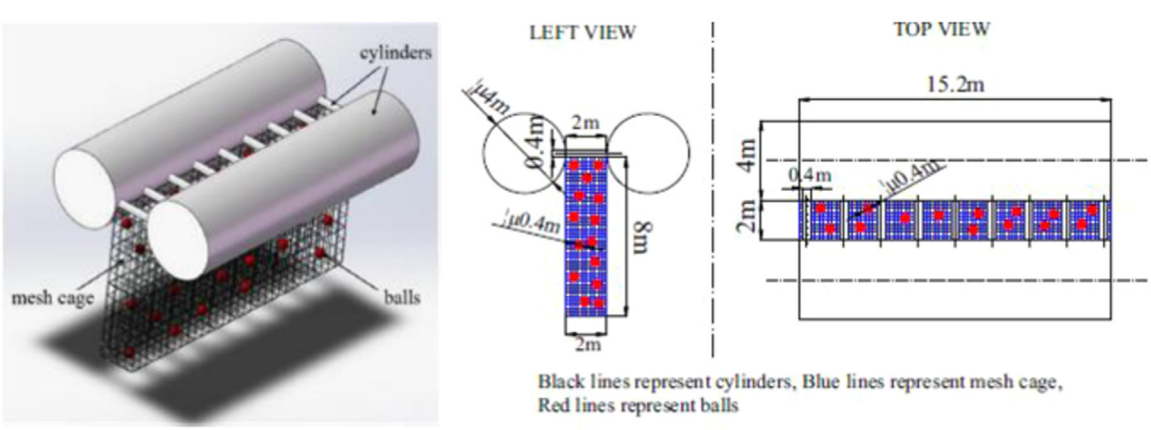

Fig. 1. The cylindrical floating breakwater with a mesh cage and balls.

balls with the diameter of 0.4 m and the density similar to water are added into the cage (Fig. 1).

3. Experiment

3.1. Experimental facilities

The model tests were conducted in the three-dimensional wave basin in the Hydraulics Modeling Laboratory of Ocean University of China (as shown in Fig. 2). The wave basin is 60 m long, 36 m wide and 1.5 m deep. But in the present experiment, only the length of 45 m length can be used, while the rest length of 15 m is the sand beach. The wave basin is equipped with a 33.75 m hinged plate wave generator, which can make both the regular and irregular waves through a computer. In the present study, all the incident waves are regular wave and the test duration is 90 s. In the opposite end, there is a wave-absorbing beach, which is stabilized by an armor layer, to reduce wave reflection. The slope of the wave-absorbing beach is 1:5.

In order to measure the free surface elevation of the wave basin, 5 wave gauges (WGs) are used to measure the incident waves and transmitted waves and the location of them can be found in Fig. 3. The distance between WG1, WG2, WG3, WG4, WG5 and the *x*-axis is 10 m, 5.31 m, 5 m, 10 m and 10.31 m respectively. WG1is used to measure incident wave, WG2 and WG3 are used to separate the incident wave and the reflected wave from the measured two waves while WG4 and WG5 are used to separate the transmitted wave by means of the two measured waves. In order to measure the motion responses, a 6-DOF measure system was applied, which includes a 6-DOF camera and three luminous. The distance between the *x*-axis and the 6-DOF camera is 4 m. Three luminous sources were installed in the middle of the cylindrical floating breakwater system, so that the camera can receive signals from these sources. The motion trail of the three luminous represents the actual motion of floating breakwater units.

3.2. Experimental floating breakwater

Considering the size of the wave basin and the wave frequency range that can be generated by wave generator controlled by a computer, the model is made based on geometrical similarity with scale factor of 1:40. In the present study, we make some adjustments in the dimensions for the traditional cylindrical FB with a mesh cage and balls, mentioned in Ji et al. (2015), to be the experimental models. The same cross section of the cylindrical FB proposed in Ji et al. (2015) is used in this paper. The floating breakwater system (as shown in Fig. 3) consists of 10 cylindrical floating breakwaters units

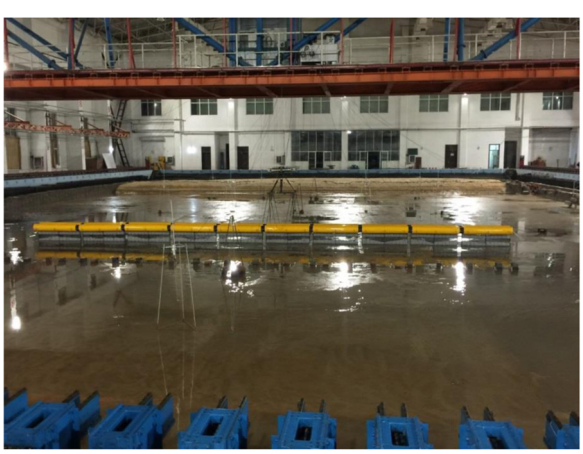

Fig. 2. Hydraulics Modeling Laboratory of Ocean University of China.

connected by 18 elastic connectors and 36 chains (as shown in Fig. 5), as well as 10 mesh cages with balls in them (Fig. 4).

The cylindrical FB has two 0.25 m (diameter)*1.5 m (length) cylinders and thirteen 0.03 m (dimeter)*0.125 m (length) cylinders. In addition, it includes a 1.5 m long, 0.125 m wide and 0.5 m high mesh cage hanging below the main structure too. 1520 rubber balls with 3.4 cm diameter are pre-placed into every mesh cages to dissipate the wave energy.

The length of the connector is 0.125 m. These connectors are made from rubber whose density is 1300 kg/m³, and include three components: two small inter cylinders and one outer hollow cylinder. Two inner cylinders are nailed into the units' cross-section and wrapped by the outer rubber cylinder. Those connectors are used mainly to absorb pitch moment and restrain the collision of two units. Due to the large stiffness of the rubber (similar material as tire), the relative motion on surge, sway, heave and roll between two adjacent units can be negligible. However, it allows the relative pitch and yaw motion, which can transfer wave energy to the elastic potential energy.

Between every two units, two chains are hinged to reinforce the connection. The total length of the floating breakwater system is 16.125 m. The main parameters of the experimental module are listed in Table 1. In the present study, we choose 90° to represent beam sea condition and 67.5° to represent oblique waves.

The structures were modeled according to geometrical and mass similarities (mass, gravity center, buoyancy and mass moment of inertia). For the mooring lines, the geometrical and mass similarities are firstly satisfied by adjusting the distribution of nuts (see Fig. 6). Elastic similarity can be achieved by adjusting the spring distribution (see Fig. 7).

By releasing the structure from several non equilibrated positions, natural modes of oscillations in 3D have been assessed in the laboratory. The natural period of oscillations of the floating breakwater system are given in Table 2.

3.3. Mooring system

The taut mooring system is used for the floating breakwater system, and 64 mooring lines are symmetrically arranged alongside the floating breakwaters, as shown in Fig. 3. The angles between *x*-axis and the mooring lines in two terminal unites (No. 2, 63, 31, 34) are −60°, 60°, −120°, 120° respectively. The length of each mooring line is 3.875 m. Each mooring line consists of three components: chain-rope-chain. The length of the chains in the lower and upper end of the mooring lines is 0.5 *m,* while the length of the rope is 2.875 m, as shown in Fig. 6. Besides, the springs and nuts (as shown in Fig. 7) are used to adjust the stiffness and weight of the mooring lines respectively. The main parameters of the mooring lines are listed in Table 3 and the axial rigidity of the chains and ropes can be measured by experiments.

3.4. Experimental conditions

The experiments were carried out in both oblique and beam sea conditions. The water depth during the model tests is 1.0 m. At beam sea condition, *y*-axis of the floating system is parallel to the wave propagation direction (as shown in Fig. 8) while the angle between *y*-axis and the wave direction is 22.5° (as shown in Fig. 9) at the oblique wave condition. Considering the environmental parameters in South China Sea, 44 wave conditions with different wave height and period are taken into consideration in both oblique and beam wave. Table 4 shows the parameters of the regular waves. Fig. 10 describes the six-degree of freedom movement for floating breakwater.

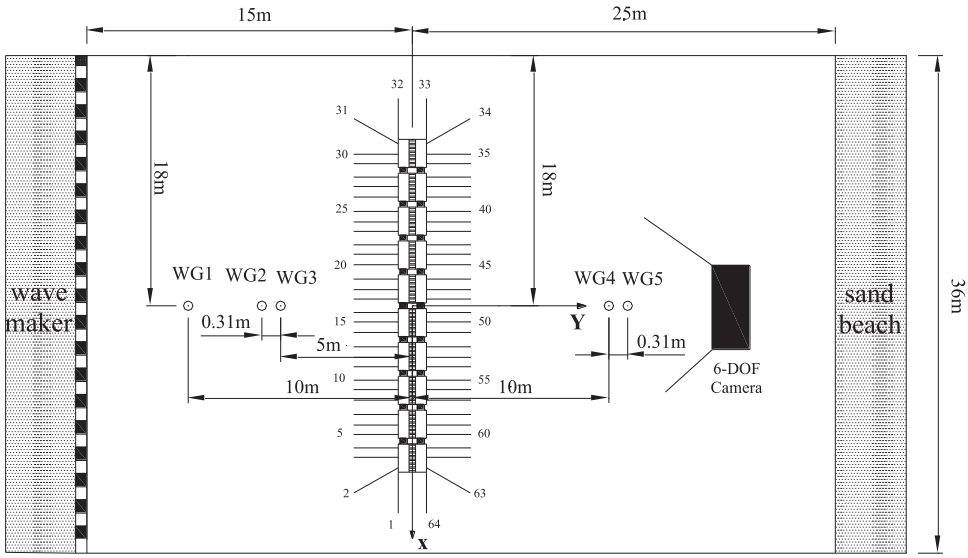

Fig. 3. Sketch of floating breakwater.

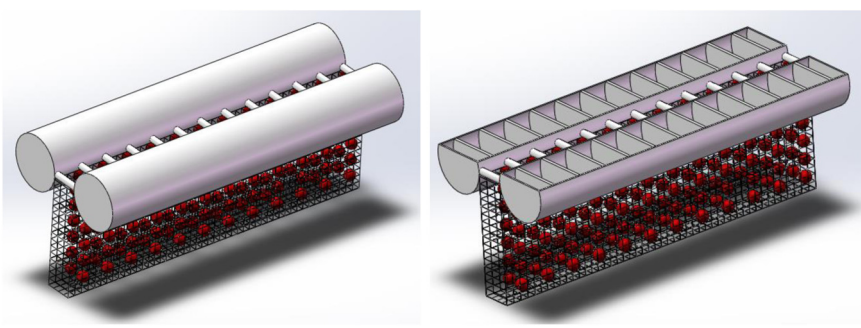

Fig. 4. The floating breakwater.

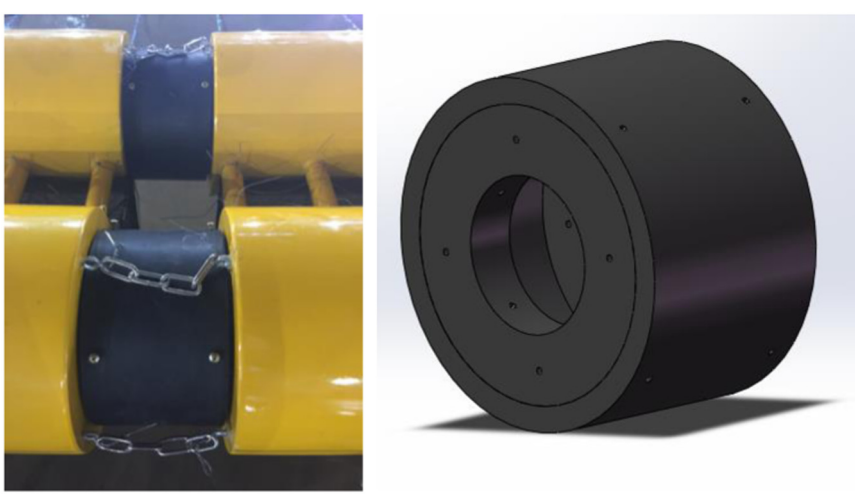

Fig. 5. Connectors between modules and chains between modules.

4. Analysis method

Goda and Suzuki (1976) proposed a two-point method to separate the reflected waves and the incident waves with the same wave period by examining the measured wave heights. The method can be used for both regular and irregular waves. In the present experiment, WG2 and WG3 are used to separate the incident and reflected waves in front of the floating system to obtain the amplitude A_i and A_r, while WG4 and WG5 are used to separate the transmitted wave after the floating system to obtain the amplitude A_t. Reflection coefficient K_r, transmission coefficient K_t and dissipation coefficient E_d can be expressed as:

Table 1
Main parameters of cylindrical floating breakwater.

Length(m)	l	1.5
Breadth(m)	B	0.625
Height(m)	h	0.25
Draft(m)	d	0.125
Mass(kg)	M	70.03
Gravity center above bottom(m)	t	0.125
Roll inertia(kg*m^2)	I_{xx}	3.22
Pitch inertia(kg*m^2)	I_{yy}	14.25
Yaw inertia(kg*m^2)	I_{zz}	16.63

Fig. 6. Three parts of the mooring line.

Fig. 7. Experimental spring.

Table 2
Natural period of motions (L is the wave length and B is the breadth of FB unit).

DOF	Surge	Sway	Heave	Roll	Pitch	Yaw
Period (s)	3.32	1.42	1.47	0.92	1.26	4.74
L/B	15.62	4.88	5.18	2.11	3.92	23.05

$$K_r = A_r / A_i \tag{1}$$

Table 3
Main parameters of the mooring lines.

	Diameter (mm)	Length (m)	Axial rigidity (KN)	The submerged weight per unit length (g^*m^{-1})
Chains	3.875	0.5	27.53	254
Rope	4.25	2.875	5.47	48.3
Chains	3.875	0.5	27.53	254

$$K_t = A_t / A_i \tag{2}$$

$$E_d = \sqrt{1 - K_r^2 - K_t^2} \tag{3}$$

As for the 6-DOF motion responses, the time domain analysis is used. The motion amplitude of the floating breakwater is defined as the oscillation amplitude relative to its mean position in waves. For example,

surge amplitude = (maximum surge amplitude-minimum surge amplitude)/2.

In fact, the majority of data are valid despite that there are few data which was subjected to signal interference. However, those interfered data will not be used in this paper.

5. Results and discussions

5.1. Wave transmission coefficients

The efficiency of wave dissipation of the floating breakwater system is estimated by its wave transmission coefficient K_t. Fig. 11 shows the wave transmission coefficients of the system in beam and oblique waves with different wavelengths. The x-axis of the figure is the nondimensionalized wavelength L/B, where L is the wavelength and B is the breadth of the floating breakwater system. It can be observed from Fig. 11 that both in beam and oblique wave conditions, the K_t curves have a similar trend with each other. As the wavelength increases, K_t increases almost linearly against wavelength at $L/B < 6.5$. It reaches its peak at $L/B = 6.5$ for all three different wave heights. Afterward, as L/B becomes larger than 6.5, the wave transmission coefficients turn to have downward trend against wavelength. This is a very interesting finding which has not been demonstrated in the published results. In the previous literatures, the breakwater has very poor behavior as the wave length becomes very large. However, some results from the motions support this finding. For example, the heave, pitch and yaw motion amplitude keep increase as $L/B > 6.5$. The large amplitude oscillating of the breakwater disperses more energy, which could be one of the reason why a downward trend of K_t can be found when $L/B > 6.5$. Of course, a detail study about the wave transmission in long waves is desired both in numerical and theoretical method. It can also be observed from Fig. 11 that at $H/h = 0.32$ (where H/h is the ratio of wave height to FB height), the wave transmission coefficient of the FB is larger than that of the other two values of H/h. But it does not mean the smaller H/h can transmit more wave energy.

Fig. 12 shows the wave transmission coefficients of the system in beam and oblique waves with different wave heights, where the wave height is nondimensionalized by the height of the floating cylinder. Two typical wavelengths ($L/B = 2.5$ and $L/B = 6$) are selected in order to investigate the effect of wave heights. Generally, the effect of wave height on wave transmission is not very evident. In short waves ($L/B = 2.5$), more wave energy can be transmitted when the wave height is small. As the wave height increases, K_t has a slight downward trend, which indicates that the FB system

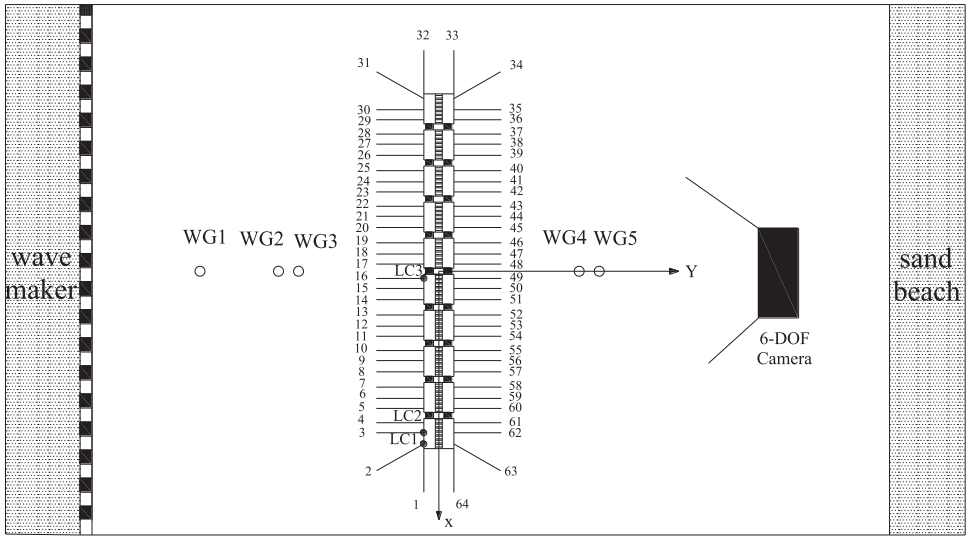

Fig. 8. Beam regular wave, $\beta=0°$.

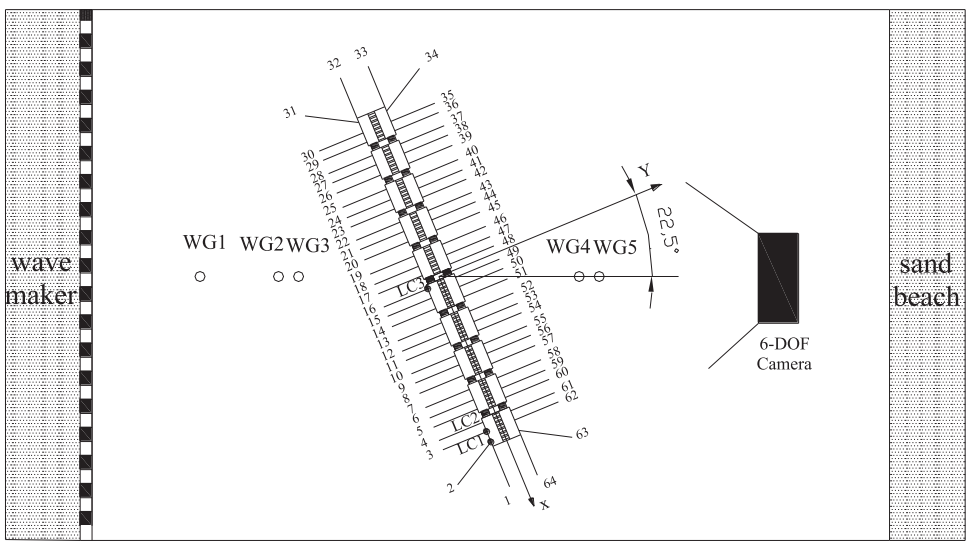

Fig. 9. Oblique regular wave, $\beta=22.5°$.

Table 4
Parameters of the regular wave condition.

	Wave height H/m	Wave period T/s	wave incident angle β (°)
A1-A12	0.08	0.8–1.9 with step at0.1	0, 22.5
A13-A22	0.15	1.0–1.9 with step at 0.1	0, 22.5
A23-A30	0.25	1.2–1.9 with step at 0.1	0, 22.5
A31-A35	0.08–0.16 with step at 0.02	1	0, 22.5
A36-A44	0.10–0.26 with step at 0.02	1.6	0, 22.5

has better performance in short waves with larger wave heights. However, due to the limitation of the wave-maker, we cannot extend the wave height to any larger values. On the other hand, in short waves, when the ratio of wave height to wavelength is very large, the waves will be determined by the nonlinear theory, which is beyond our consideration. In long waves ($L/B=6$), the

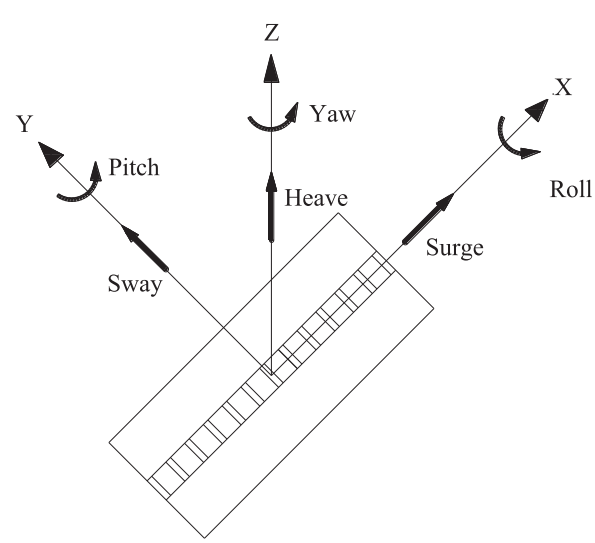

Fig. 10. 6-degree of freedom motion for floating breakwater module.

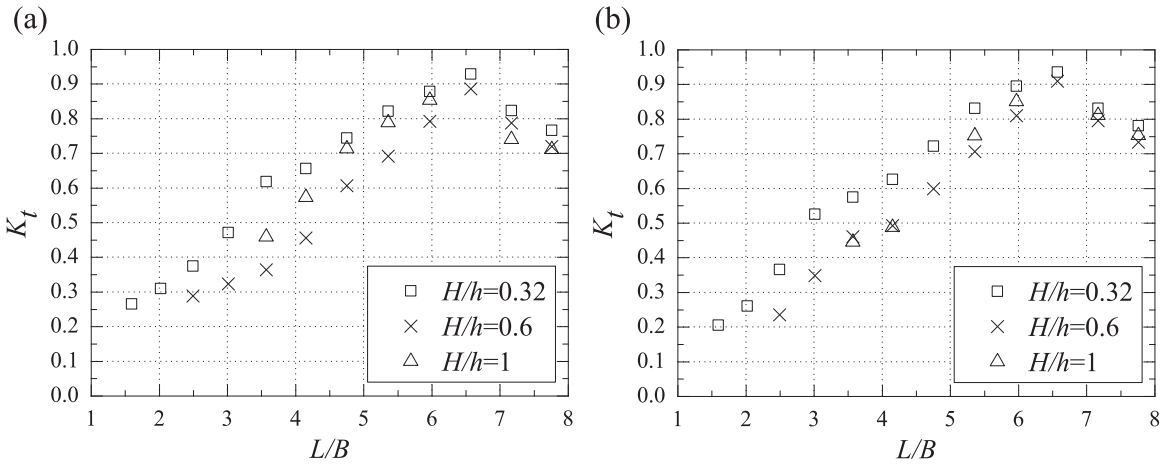

Fig. 11. Transmission coefficients of FB system in waves with different wavelengths. (a) Beam wave condition; (b) oblique wave condition.

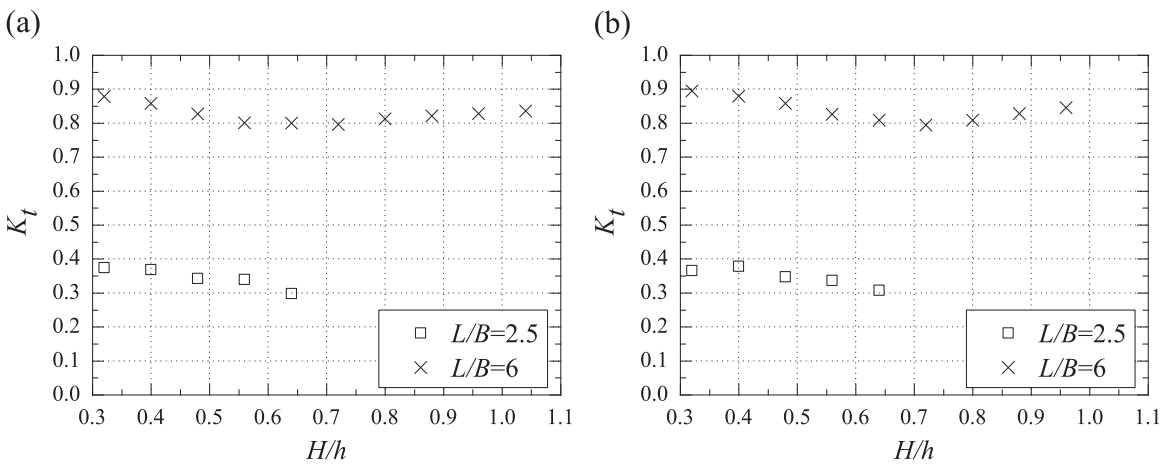

Fig. 12. Transmission coefficients of FB system in waves with different wave heights. (a) Beam wave condition; (b) oblique wave condition.

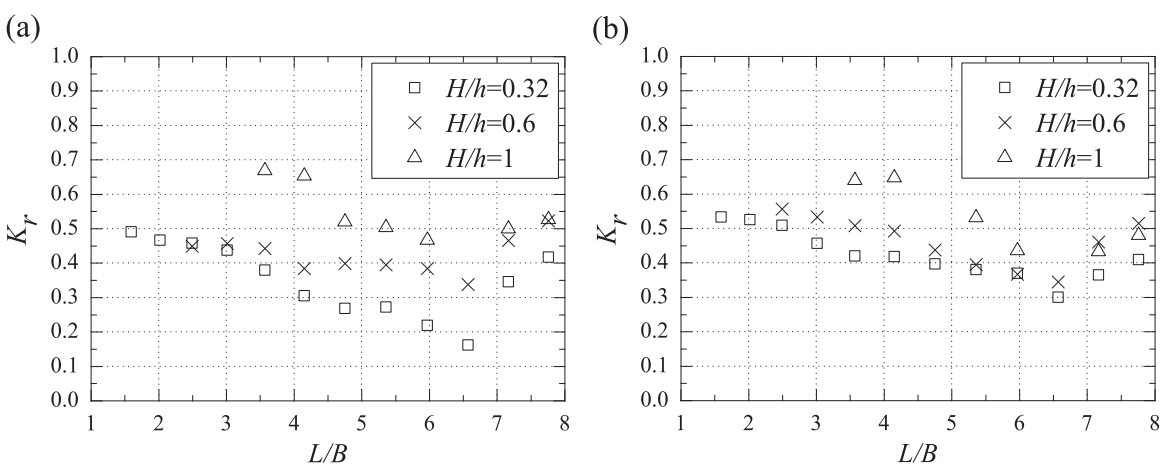

Fig. 13. Reflection coefficients of FB system in waves with different wavelengths. (a) Beam wave condition; (b) oblique wave condition.

wave transmission coefficients are much larger than those in short waves in the full range of wave heights. As the wave height increase, the K_t has a slight downward trend until it reaches its minimum value at $H/h=0.7$, followed by a slight upward trend. However, the minimum wave transmission coefficient is 0.8, which is still very large in long waves.

It can be concluded from Fig. 11 and Fig. 12 that the cylindrical breakwater system is able to reflect most of the short waves. Therefore, it is very effective in short wave condition for a wide range of wave heights. In case of long waves, most of the wave energy is transmitted. As the wavelength keeps increasing, the transmission coefficient will drop down. This is a desirable phenomenon especially when the breadth of the FB is small. In this case, the wavelength to breadth ratio could be very large (probably it can exceed the ratio where the peak K_t is achieved) and the efficiency of the FB is still satisfactory. However, the maximum wavelength to breadth ratio L/B in the present experiment is less than 8 due to the large breadth of the present FB model. A further

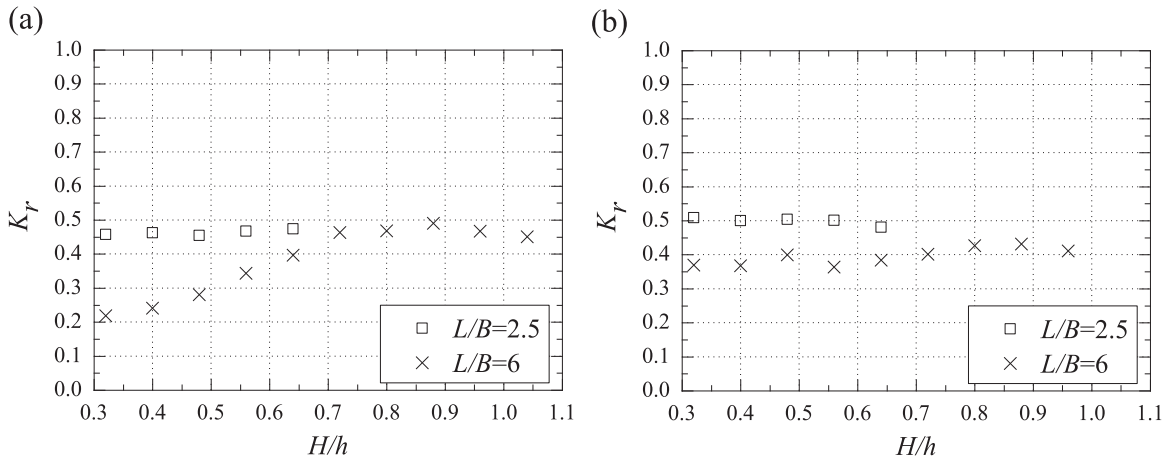

Fig. 14. Reflection coefficients of FB system in waves with different wave heights. (a) Beam wave condition; (b) oblique wave condition.

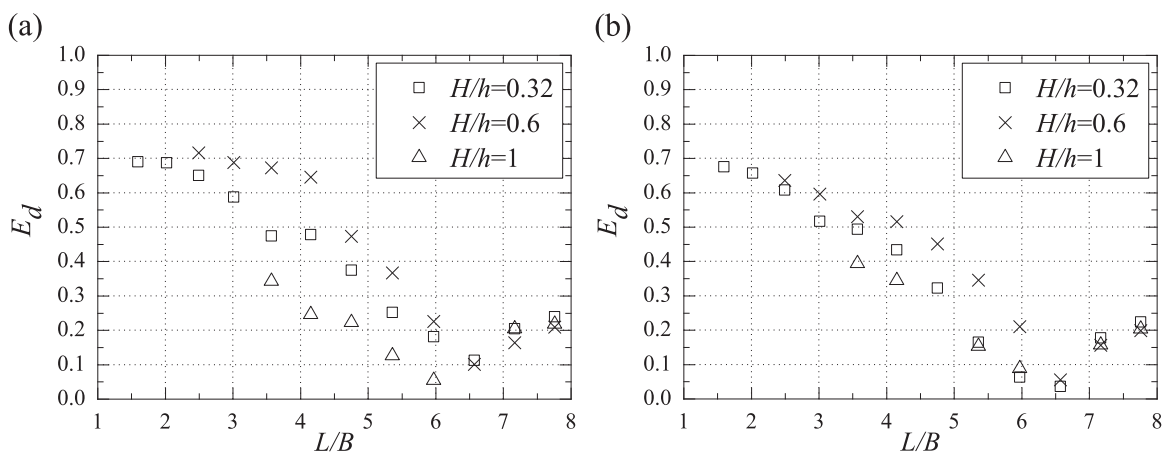

Fig. 15. Dissipation coefficients of FB system in waves with different wavelengths. (a) Beam wave condition; (b) oblique wave condition.

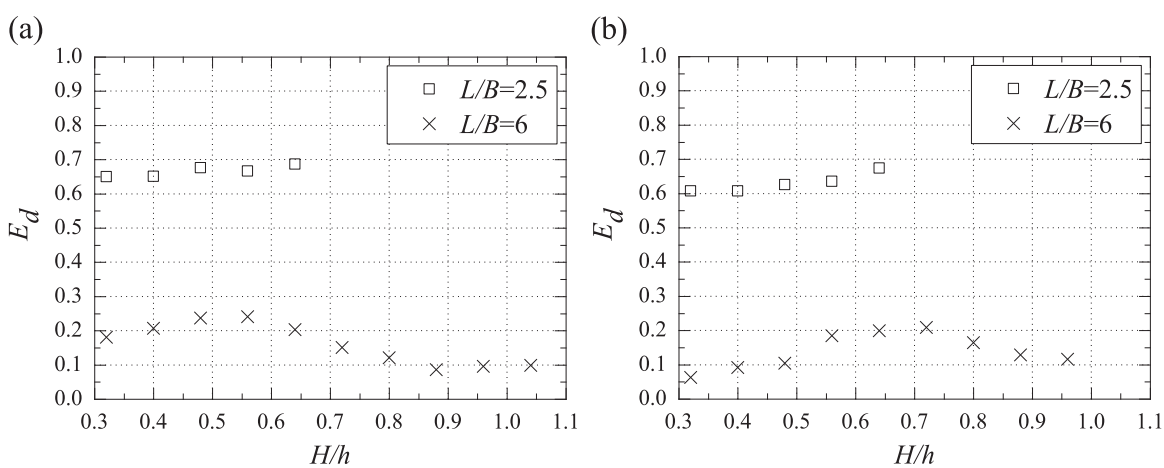

Fig. 16. Dissipation coefficients of FB system in waves with different wave heights. (a) Beam wave condition; (b) oblique wave condition.

investigation of $L/B > 8$ will be carried out in the future to see the range of this downward trend. With regard to the incident wave angle, the difference of the wave transmission coefficient is very small between the beam and oblique conditions. It indicates the present FB system has a satisfactory performance both in beam and oblique wave conditions.

5.2. Wave energy reflection coefficients

Wave reflection is an important way for the floating breakwaters to attenuate the wave energy. Fig. 13 shows the wave reflection coefficients of the system in beam and oblique waves with different wavelengths. It can be observed from Fig. 13 that the trend of the K_r curves is consistent in both beam and oblique wave conditions. At $L/B < 6.5$, the wave reflection coefficient curves generally keep a downward trend. But the slopes of the curves of different wave height are various. In beam waves, K_r curves decease rapidly with the increase of the wavelength at $H/h = 0.32$ and $H/h = 1$. But the drop of K_r curves at $H/h = 0.6$ is not very obvious. With regard to the oblique wave condition, the downward

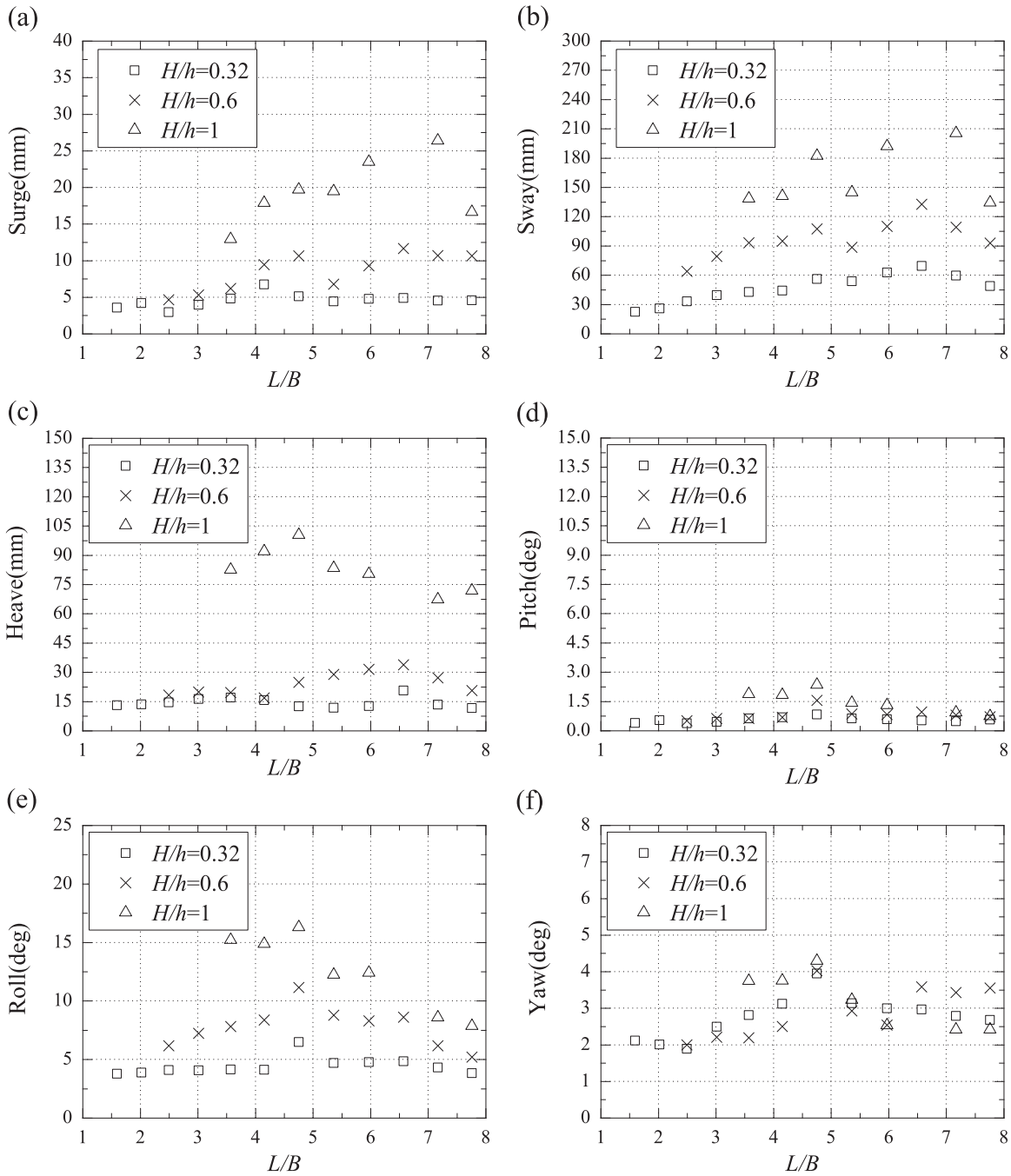

Fig. 17. 6-DOF motion responses of floating breakwater against wavelength in beam waves. (a) Surge motion; (b) sway motion; (c) heave motion; (d) pitch motion; (e) roll motion; (f) yaw motion.

trend of K_r curves is mild. However, the wave reflection coefficients turn to increase after they reach their minimum value at $L/B=6.5$. It is most possibly due to the severe sway motion, which can reduce the wave reflection. It can be found that the sway motion gets the peak response at $L/B=6.5$ in Fig. 17(b). It also shows that the wave transmission coefficient gets the largest value when the wave reflection coefficient gets the smallest value by comparing Fig. 13 with Fig. 14. So it can be concluded that the motion period of the sway of the FB is very important to the wave attenuation effectiveness and it can be obtained by Table 2. It can also be observed from Fig. 13 that at $H/h=1$, the wave reflection coefficient of the FB is larger than that of the other two values of H/h. It means the larger H/h the more waves can be reflected by the floating breakwater system.

Fig. 14 shows the wave reflection coefficients of the system in beam and oblique waves with different wave heights. It can be observed that the effect of wave height on reflection coefficients is not very evident for short waves ($L/B=2.5$) in both beam sea and oblique sea conditions. However, in the long waves ($L/B=6$), the reflection coefficients in beam waves are quite different from those in oblique waves. In beam waves, the reflection coefficients increase significantly with the increase of the wave height before reaching its peak at $H/h=0.88$. Afterward, as H/h becomes larger than 0.88, the wave reflection coefficients keep stable. In oblique waves, as wave height increases, reflection coefficients keep a slow growth.

It can be concluded from Fig. 13 and Fig. 14 that the wave reflection coefficients in oblique waves are larger than these in beam

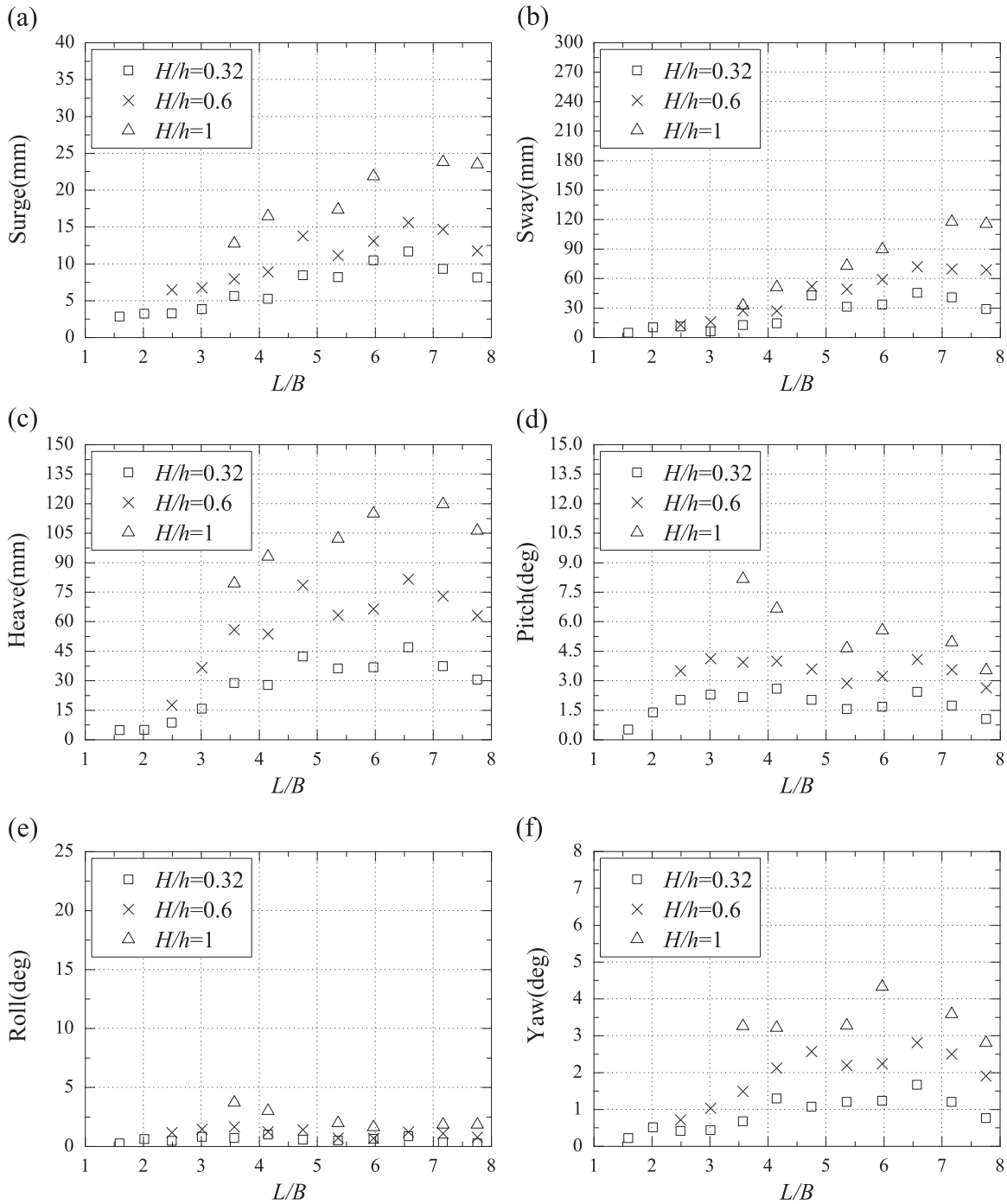

Fig. 18. 6-DOF motion responses of floating breakwater against wavelength in oblique waves. (a) Surge motion; (b) sway motion; (c) heave motion; (d) pitch motion; (e) roll motion; (f) yaw motion.

waves, which indicates that the present FB system has a better performance in reflecting waves in oblique wave condition.

5.3. Wave energy dissipation coefficients

Fig. 15 shows the wave dissipation coefficients of the system in beam and oblique waves with different wavelengths. It can be observed from Fig. 15 that both in beam and oblique wave conditions, the E_d curves have a similar trend with each other. For $L/B \leq 6$, E_d decreases rapidly as the wavelength increases. Afterward, as wavelength increases, wave dissipation coefficient has a slight growth for $L/B \geq 6.57$. This can be explained by the motion responses of the system. The motion responses of the floating breakwater in 6 DOF all experience a trend of decrease at $L/B \geq 6.57$ (as shown in Fig. 17 and Fig. 18). In addition, for all wave conditions, wave dissipation coefficients E_d at $H/h=0.6$ is greater than the other two wave heights while the smallest E_d is observed at $H/h=1$.

Fig. 16 shows the wave dissipation coefficients E_d as a function of wave heights in terms of H/h, ranging from 0.3 to 1.1. Two typical wavelengths are selected to be studied. It is obvious that wave dissipation coefficient for short wave ($L/B=2.5$) is much greater than that for long wave ($L/B=6.0$). In short waves ($L/B=2.5$), wave dissipation coefficients E_d only have a slight growth with the increase of wave height. In long wave ($L/B=6.0$), E_d increases until it reaches its peak, followed by a slight decrease.

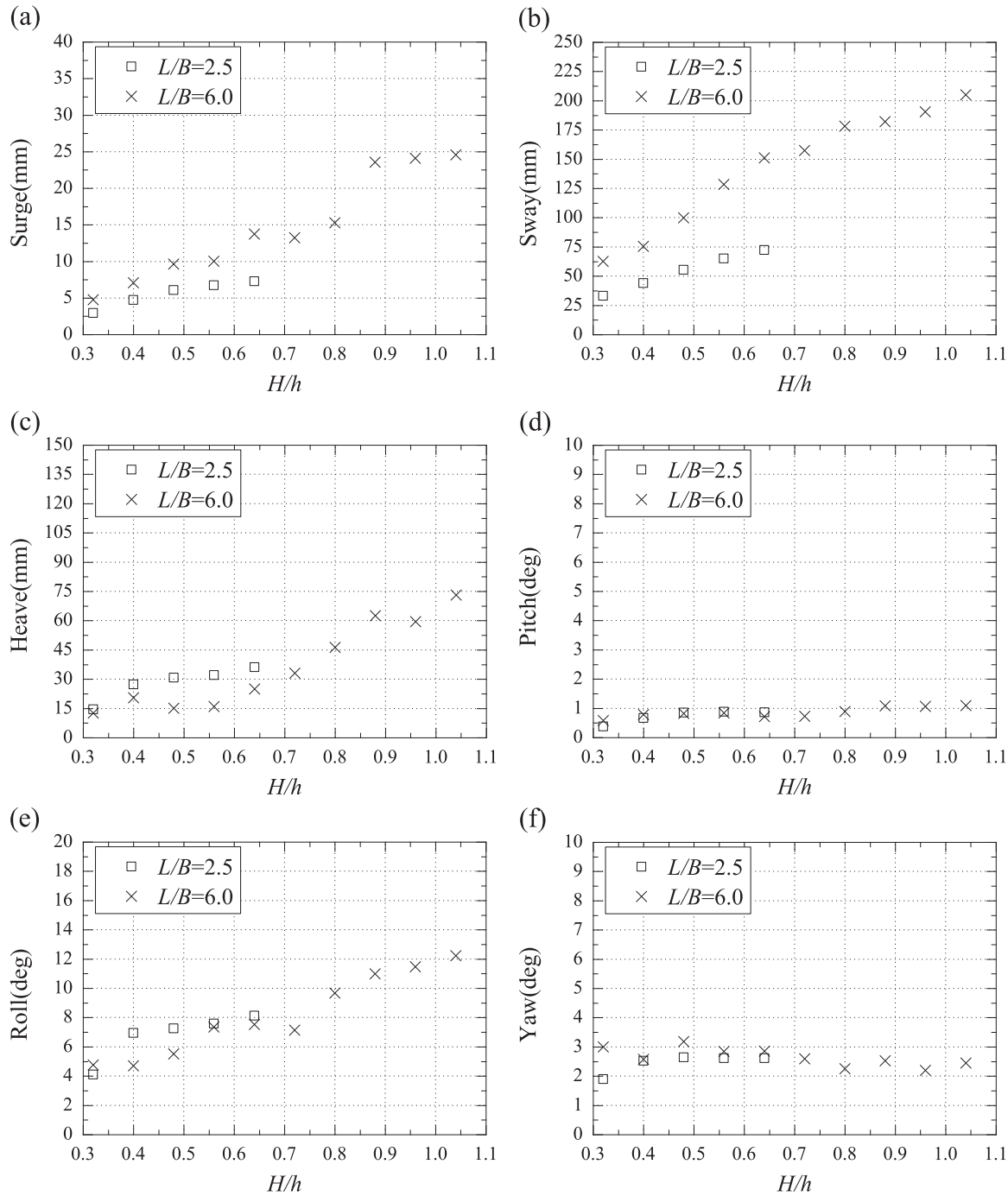

Fig. 19. 6-DOF motion responses of floating breakwater against wave height in beam waves. (a) Surge motion; (b) sway motion; (c) heave motion; (d)pitch motion; (e)roll motion; (f)yaw motion.

However, the peak value in beam waves appears at $H/h=0.55$, while in oblique wave, it turns to be at $H/h=0.7$.

5.4. Motion responses

Fig. 17 shows the relationship between module's six-degree of freedom motion responses and wavelength in beam waves. In case of three translational motions (surge, sway and heave motion), there is a spike appears at $L/B=4.76$ for surge and sway. Due to the incident wave angle, the sway in beam waves has the largest amplitude. And at $L/B=6.57$, the sway motion achieves a very large value. However, the peaks at $L/B=4.76$ and 6.57 are not due to the natural frequencies. Of course, the natural frequency is very important for a floating body. The peaks of the motion responses can be determined by two factors: the natural frequency and the external forces. From Table 2 we can see that the natural frequencies in 6 DOF could not be the same. However, the two peaks of surge, sway and yaw motion appear at the same frequencies ($L/B=4.76$ and 6.57). It is believed that these frequencies are not the natural frequencies of any degrees of motion. We exam the forces on the mooring lines and find these frequencies correspond to the maximum forces, which means the peaks of the motion of the FB system are determined by the external forces. Actually, this is also the case for some floating platforms, where the peaks of motion are determined by the peaks of the wave exciting forces. For three rotational motions, roll motion plays a key role compared with

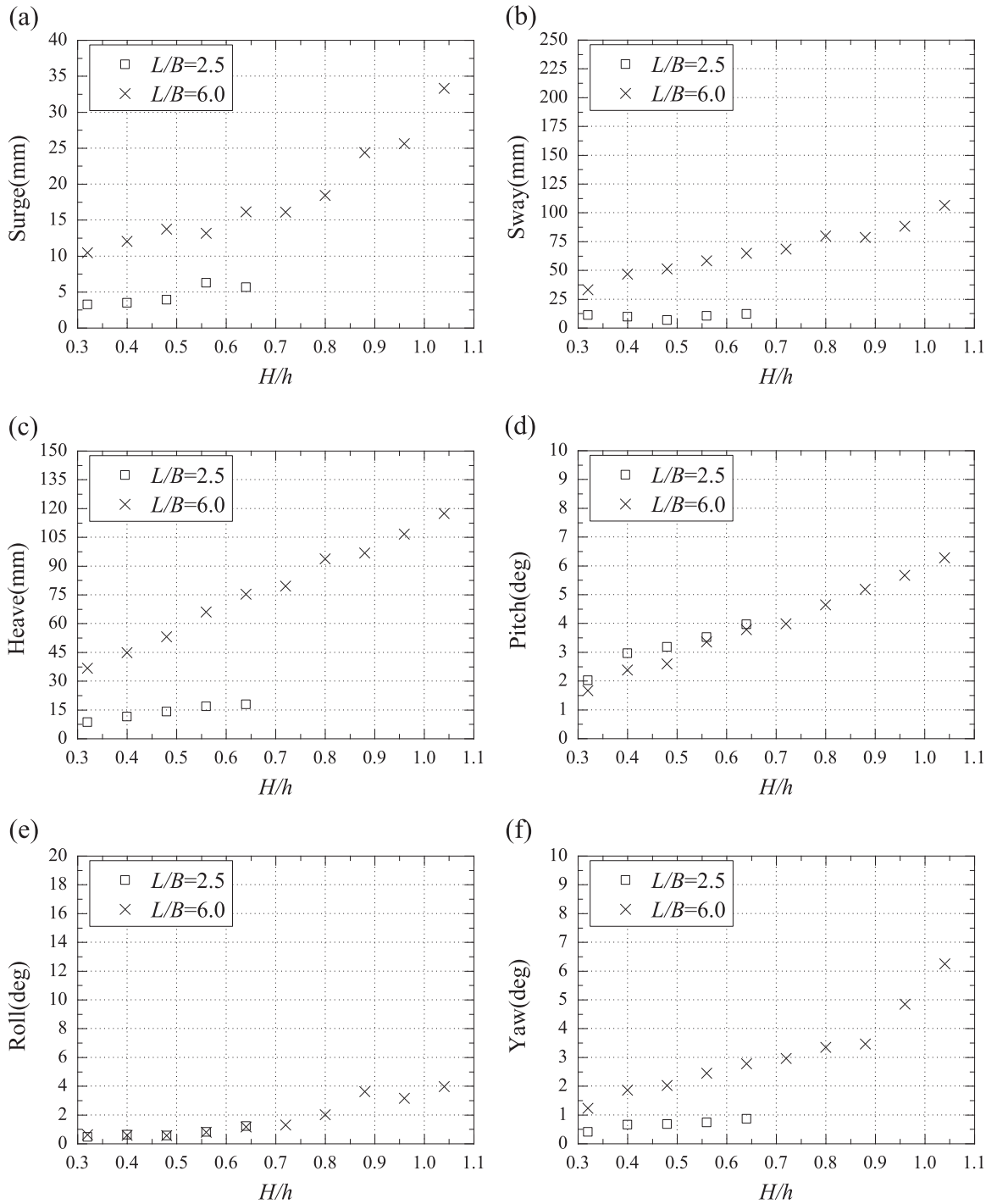

Fig. 20. 6-DOF motion responses of floating breakwater against wave height in oblique waves. (a) Surge motion; (b) sway motion; (c) heave motion; (d)pitch motion; (e)roll motion; (f)yaw motion.

two others in beam waves. It can be seen from Fig. 17(e) that the amplitude of roll motion grows until $L/B=4.76$ and then followed by a downward trend. It is expected that the surge, pitch and yaw motion should be zero due to the incident wave condition. However, due to the coupled behaviors between the FB units and between the FB floaters and mooring lines, these degrees of motion are still noticeable. However, the amplitudes of these degrees of motions are relatively small compare the rest of the degrees of motion.

Fig. 18 shows the motion responses against the wavelength in oblique waves. Generally, the conclusions in oblique waves are similar to these in beam waves. There are two spikes observed at $L/B=4.76$ and 6.57 respectively.

Fig. 19 shows the motion responses against the wave height in beam waves. Based on linear assumption, the motion responses are expected to have a linear relation with the wave height. But this linear relation has not been observed from Fig. 19. With regard to the surge, heave and sway motions, which are most violate in beam sea waves, the motion amplitudes increase nonlinearly against the wave amplitude. This nonlinear results is due to the large amplitude of the incoming waves. And this nonlinear relation is most obvious at wave height range of $0.6 < H/h < 0.8$.

Compared with the nonlinearity in beam waves, only a weakly nonlinear phenomenon can be observed in oblique wave condition

except yaw and surge response, as shown in Fig. 20. At wave height range of $H/h > 0.9$, the yaw response amplitude increases dramatically. With regard to the three translational motions, the motion response amplitude at large wavelength is much larger than that at short waves. But this conclusion cannot cover the pitch and roll motions.

6. Conclusion

In the present paper, we conducted a 3D experiment to investigate an innovative floating breakwater system. The performance of the FB system was estimated by measuring the wave transmission coefficients, wave dissipation coefficients and six-degree of freedom motion responses. These measurements are influenced by the factors of wavelength, wave height and incident wave angle. According the experimental measurements, some conclusions are shown as follows:

(1) The proposed cylindrical floating breakwater system is able to dissipate most of the short waves in both beam and oblique wave conditions. In case of long waves, most of the wave energy is transmitted. As the wavelength keeps increasing, the transmission coefficient will drop down. This is a desirable phenomenon for the engineering practice, especially when the breadth of the FB is small.
(2) With the increase of the wavelength, the motion response amplitude of the FB system suffers an increase before it reaches its peak value, followed by a decrease trend. As the wave amplitude increases, the motion response amplitude increases nonlinearly due to the nonlinearity of the large amplitude incident waves and coupled behavior between the FB units and mooring lines. The sway period of the FB is very important to the wave attenuation effectiveness In order to ensure the wave attenuation effectiveness, the sway period of the FB should be designed to avoid the most possible wave frequency at certain sea condition.

In summary, by examining the wave transmission coefficients and the motion responses, it can be concluded that the proposed FB system has a satisfactory performance and it can be used to a wide range of sea conditions, including South China Sea.

Acknowledgments

This study was supported financially by the National Natural Science Foundation of China (Grant no.51379095) and the National Basic Research Program of China (973 Program; Grant no.2013CB3610 0).

Appendix A. Supplementary material

Supplementary data associated with this article can be found in the online version at http://dx.doi.org/10.1016/j.oceaneng.2016.07.051.

References

Abul-Azm, A.G., Gesraha, M.R., 2000. Approximation to the hydrodynamics of floating pontoons under oblique waves. Ocean Eng. 27 (4), 365–384.
Arunachalam, V.M., Raman, H., 1982. Experimental studies on a perforated horizontal floating plate breakwater. Ocean Eng. 9 (1), 35–45.
Bayram, A., 2000. Experimental study of a sloping float breakwater. Ocean Eng. 27 (4), 445–453.
Chen, Z.J., Wang, Y.X., Dong, H.Y., Zheng, B.X., 2012. Time-domain hydrodynamic analysis of pontoon-plate floating breakwater. Water Sci. Eng. 5 (3), 291-30.
Dong, G.H., Zheng, Y.N., Li, Y.C., Teng, B., Guan, C.T., Lin, D.F., 2008. Experiments on wave transmission coefficients of floating breakwaters. Ocean Eng. 35, 931–938.
Gesraha, M.R., 2006. Analysis of Π shaped floating breakwater in oblique waves: I. Impervious rigid wave boards. Appl. Ocean Res. 28 (5), 327–338.
Goda, Y., Suzuki, Y., 1976. Estimation of incident and reflected waves in random wave experiments. In: Proceedings of the 15th International Conference on Coastal Engineering. ASCE. pp. 828–845.
Hanif, M., 1983. Analysis of heaving and swaying motion of a floating breakwater by finite element method. Ocean Eng. 10 (3), 181–190.
He, F., Huang, Z., Law, A.W., 2012. Hydrodynamic performance of a rectangular floating breakwater with and without pneumatic chambers: an experimental study. Ocean Eng. 51, 16–27.
Ji, C.Y., Chen, X., Cui, J., et al., 2015. Experimental study of a new type of floating breakwater. Ocean Eng. 105, 295–303.
Koraim, A.S., 2015. Mathematical study for analyzing caisson breakwater supported by two rows of piles. Ocean Eng. 104, 89–106.
Koraim, A.S., Rageh, O.S., 2013. Effect of Under Connected Plates on the Hydrodynamic Efficiency of the Floating Breakwater. Ocean Eng. 28 (3), 349–362.
Loukogeorgaki, E., Michailides, C., Angelides, D.C., 2012. Hydroelastic analysis of a flexible mat-shaped floating breakwater under oblique wave action. J. Fluids Struct. 31, 103–124.
Loukogeorgaki, E., Yagci, O., Kabdasli, M.S., 2014. 3D Experimental investigation of the structural response and the effectiveness of a moored floating breakwater with flexibly connected modules. Costa. Eng. 91, 164–180.
Martinelli, L., Ruol, P., Zanuttigh, B., 2008. Wave basin experiments on floating breakwaters with different layouts. Appl. Ocean Res. 20, 199–207.
McCartney, B.L., 1985. Floating breakwater design. J. Waterw., Port., Coast., Ocean Eng. 111 (2), 304–317.
Najafi-Jilani, A., Rezaie-Mazyak, A., 2011. Numerical investigation of floating breakwater movement using SPH method. J. Nav. Archit. Ocean Eng. 3, 122–125.
Ozeren, Y., Wren, D.G., Altinakar, M.S., Work, P.A., 2011. Experimental investigation of cylindrical floating breakwater performance with various mooring configurations. J. Waterw. Port. Coast. Ocean Eng. 137 (6), 300–309.
Peña, E., Ferreras, J., Sanchez-Tembleque, F., 2011. Experimental study on wave transmission coefficient, mooring lines and module connector forces with different designs of floating breakwaters. Ocean Eng. 38, 1150–1160.
Peng, W., Lee, K.H., Shin, S.H., Mizutani, N., 2013. Numerical simulation of interactions between water waves and inclined-moored submerged floating breakwaters. Coast. Eng. 82, 76–87.
Ragih, O.S., El-Alfy, K.S., Shamaa, M.T., Diab, R.M., 2006. An experimental study of spherical floating bodies under waves, In: Proceedings of 10th International Water Technology Conference (IWTC10), Alexandria, Egypt, pp. 357–375.
Rahman, M.A., Mizutani, N., Kawasaki, K., 2006. Numerical modeling of dynamic responses and mooring forces of submerged floating breakwater. Coast. Eng. 53, 799–815.
Sannasiraj, S.A., Sundar, V., Sundaravadivelu, R., 1995. The hydrodynamic behavior of long floating structures in directional seas. Appl. Ocean Res. 17 (4), 233–243.
Sannasiraj, S.A., Sundar, V., Sundaravadivelu, R., 1998. Mooring forces and motion responses of pontoon-type floating breakwaters. Ocean Eng. 25 (1), 27–48.
Stamos, D.G., Hajj, M.R., Telionis, D.P., 2003. Performance of hemi-cylindrical and rectangular submerged breakwaters. Ocean Eng. 30 (6), 813–828.
Wang, H.Y., Sun, Z.C., 2010. Experimental study of a porous floating breakwater. Ocean Eng. 37, 520–527.
Williams, A.N., Abul-Azm, A.G., 1997. Dual pontoon floating breakwater. Ocean Eng. 24 (5), 465–478.
Zheng, Y.H., Shen, Y.M., You, Y.G., Wu, B.J., Jie, D.S., 2006. Wave radiation by a floating rectangular structure in oblique seas. Ocean Eng. 33 (1), 59–81.